Statistical analysis on the removal of malachite green dye using active carbons of *Achyranthes aspera* and *Allamanda blanchetii* plants

Sujitha Ravulapalli and Ravindhranath Kunta*

Department of Chemistry, Koneru Lakshmaiah Education Foundation, Green Fields, Vaddeswaram-522 502, Guntur Dt., A.P., India

*Corresponding author. E-mail: ravindhranath.kunta@gmail.com

Abstract

Activated carbons were prepared from the stem parts of *Achyranthes aspera* and *Allamanda blanchetii* plants and were investigated as adsorbents for the removal of malachite green dye from contaminated water. Various extraction conditions such as pH, initial concentration of dye, adsorbent dosage, temperature, agitation time and presence of co-ions were optimized for the maximum possible extraction of the dye. For analyzing the combined effect of these parameters on the removal efficiency of the adsorbents, statistical optimization modelling was adopted. The adsorbents developed were characterized and the adsorption abilities were observed to be 40.0 mg/g and 53.0 mg/g for the active carbons of *Achyranthes aspera and Allamanda blanchetii* plants respectively. The mechanism of adsorption was studied using various isotherm models and it was found that the Freundlich model describes well the adsorption process. Thermodynamic studies revealed the endothermic and spontaneous nature of physisorption. The kinetics of adsorption were well defined by the pseudo-second-order model. Desorption and regeneration studies of the spent adsorbents indicated that the percentage of extraction has not come down below 80.0% even after five regenerations for both the adsorbents. The validity of the methods developed are tested with real dye-polluted industrial effluent samples.

Key words: achyranthes aspera plant, active carbon, adsorbent, adsorption, malachite green dye, regeneration

INTRODUCTION

Malachite Green Dye (MGD), a basic dye classified in the tri phenyl methane family, has widely been used in dyeing of leather, jute, silk, paper and wool and also in distilleries. Further, the dye is widely probed as a parasiticide, bactericide and fungicide and in many aquacultural industries globally (Zhang *et al.* 2008). The effluents from these industries, if not completely free from the dye before discharging, enter into water bodies (Uma *et al.* 2013). As the dye is non-degradable, it becomes persistent in the water steams and poses an impending environmental problem. It is highly lethal to freshwater fishes, in both acute and chronic exposures. Moreover, due to its mutagenic, carcinogenic, genotoxic effects, it causes serious public health hazards to aquatic fauna, flora and human beings (Srivastava *et al.* 2004). The clinical observations described so far reveal MGD as a 'multi-organ toxin'. It decreases the intake of food, affects the progress of growth and fertility; and also cause severe harm to heart, kidney, spleen, liver. Further, the dye imposes lesions on the lungs, skin, and also in eyes; and poses erotogenic effects (Yonar & Yonar 2010). The colored waters, besides possessing non-aesthetic nature, obstructs with the passage of sunlight into the water bodies and thereby decreases the natural photosynthetic action and disturbs the eco-systems (Ashtoukhy 2009).

Various conventional methods based on membrane separation, biodegradation, electro-coagulation, reverse osmosis, chemical oxidation, adsorption and photo degradation (Sharma *et al.* 2010) are

reported in literature for the removal of dyes form polluted waters and these methods suffer from one or the other disadvantage such as being non-economical, involving tedious procedures etc. (Yadav *et al.* 2013; Sujitha & Ravindhranath 2018a). The adsorbents derived from bio-materials are attracting the attention of the researchers in controlling various dyes. In fact, our research group made some progress in this aspect and found interesting results and they have been reported to the literature (Sujitha & Ravindhranath 2017a, 2017b, 2018b; Naga Babu *et al.* 2018).

On perusal of the literature, it is inferred that there are reports on the removal of MGD using bio-adsorbents, activated carbon of Durian seed (Mohd Azmier Ahmad *et al.* 2014), Coconut fronds (Mohammad *et al.* 2017), *Avena sativa* hull (Banerjee *et al.* 2016), *Artocarpus altilis* fruit skin (Lim *et al.* 2016), brown marine macro algae (Jerold & Sivasubramanian 2016), Lindley seed biomass (Aksakal *et al.* 2009), Biopolymer adsorbent (Sekhar *et al.* 2009), neem leaves (Odoemelam *et al.* 2018), potato plant waste (Gupta *et al.* 2011), fruit shell of tamarind (Saha *et al.* 2010b), CO_2-activated carbon derived from cattail biomass (Yu *et al.* 2017), activated carbons of epicarp of Ricinus communis (Santhi *et al.* 2010), cashew nut bark (Parthasarathy *et al.* 2011), neem sawdust (Khattri & Singh 2009) and organically modified clay (Arrellano-Cárdenas *et al.* 2013) have been employed as bio-adsorbents for the removal of MGD.

In the present investigation, we examined various plant materials as adsorbents for the removal of MGD and observed that the active carbons developed from the stems of *Allamanda blanchetii* and *Achyranthes aspera* have affinity towards MGD. In the present work investigations are made in this regard and are presented comprehensively.

MATERIALS AND METHODS

Malachite green dye:

Malachite green dye (MGD) is a cationic dye; classified as tri aryl methane dye and is widely used in pigment industries. It exists as a chloride salt, the molecular formula of MGD is [C_6H_5C (C_6H_4N ($CH_3)_2)_2$] Cl. The dye shows a strong absorption band at 618 nm and hence the intense green color results. The structural formula of MGD is shown in Figure 1.
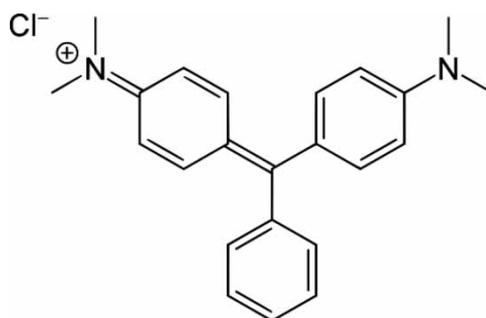

Figure 1 | Structural formula of Malachite green dye (MGD).

Plant description

Achyranthes aspera [Figure 2(a)] is a herb of the Amaranthaceae family and it grows to a height of nearly 15 cm in all parts of India. *Allamanda blanchetii* [Figure 2(b)] is a species of flowering plants, belongs to the family Apocynaceae. Allamanda plants are evergreen, erect or weakly climbing shrubs growing up to 3 meters tall. Both the plants are distributed universally all around the world especially in the southern parts of India.

Figure 2 | Plants (a) Achyranthes aspera (b) Allamanda blanchetii.

Chemicals and reagents:

All chemicals used in this work are of Analytical Reagent Grade and were purchased from Merck Pvt. Ltd.

Preparation of adsorbents:

(a) Achyranthes aspera active carbon preparation:

The cut pieces of the stems of Achyranthes aspera and *Allamanda blanchetii* plants are washed with distilled water; dried under sunlight and carbonized at 300 °C for 120 minutes in a muffle furnace. The carbons obtained were ground and sieved with 75 μm ASTM mesh and the sieved carbons were distilled water washed, filtered and oven dried at 110 °C. The carbons were activated by heating the carbon powders with 1N HNO_3 at 800C° for 3 h. Thus activated carbons were filtered and washed thoroughly with de-ionized water till the washings were neutral, oven dried (110 °C) for 4 hrs and stored in air tight bottles. Thus obtained nitric acid activated carbons prepared from the stem parts of *Achyranthes aspera* and *Allamanda blanchetii* plants are named as NACSAA and NACSAB respectively.

Equipment and characterization:

The surface morphologies of the adsorbents: NACSAA and NACSAB (before and after MGD loading) were studied to detect the possible changes on the adsorbents' surface. The Field emission scanning electron microscope (FESEM) analytical studies were made using a JEOL JSM-7600F model instrument. The SEM monographs were taken with varying resolutions at 10.0 kV.

The Fourier transform-infrared (FT-IR) spectra of the adsorbents: NACSAA and NACSAB (before and after MGD loading) and malachite green dye were noted by a FT-IR spectrophotometer of model: BRUKER ALFA in the frequency range 4,000–500 cm^{-1}.

Further, the adsorbents were characterized for various textual properties using standard procedures described elsewhere (Bureau of Indian Standards 1989; Namasivayam & Kadirvelu 1997; ASTM D4607-94 2014). The BET surface area for NACSAA and NACSAB (before and after adsorption of MGD) were measured using a nitrogen gas adsorption analyzer (computer-controlled), at 78 K (Brunauer *et al.* 1938).

Batch adsorption experiments:

Batch type adsorption studies were executed as described in previous literature (Sujitha & Ravindhranath 2018c). The dye concentration in the solution was assayed by UV-visible spectrophotometer (λ_{max}: 618 nm) as described elsewhere (American Public Health Association 1998).

The adsorption capacity (q_e), and the sorption removal efficiency (%) at a given agitation time for the adsorbent were determined by the following equations.

$$\text{Adsorption capacity: } (q_e) = \frac{(C_i - C_e)}{m} V$$

$$\text{\% removal: } (\% \, R) = \frac{(C_i - C_e)}{C_i} \, 100$$

where C_i (mg/L) is the initial concentration of MGD; m (g) is the mass of adsorbent; C_e (mg/L) is the remained dye concentration at equilibrium; V (L) is the volume of the dye solution.

The influence of the combined effects of parameters such as pH, initial dye concentration, adsorbent dose and contact time for the two adsorbents NACSAA and NACSAB were investigated and the observations are presented in Figures 5(a)–5(f) and 6(a)–6(f).

The influence of temperature on the extraction of MGD was investigated and the results are depicted in Figure 7(a) and 7(b) and Table 2. The influence of a five times excess of co-ions exist naturally in water was investigated and the results are depicted in Figure 7(c) and 7(d).

The adsorptive nature of the adsorbents NACSAA and NACSAB was investigated by using different isotherms of adsorption and models of kinetics. The results are presented in Figure 8(a)–8(h) and Tables 3 and 4.

Statistical optimization of adsorption parameters

A preliminary sensitivity analysis is carried out on the physicochemical parameters namely, pH (A), sorbent dosage (B), agitation time (C), and initial MGD concentration (D), which affect the adsorption capabilities of adsorbents. However, to analyze the combined effect of the said parameters on the removal efficiency of the adsorbents, a statistical optimization modelling was carried out using a Response Surface Method (RSM) based Central Composite Design (CCD) package of the statistical software package Design-Expert, Minneapolis, USA (Box & Hunter 1957; Sen *et al.* 2014). The empirical model is developed in terms of percentage of MGB adsorption (Y) using the CCD package, as it employs a minimum possible number of samples in optimizing the identified physicochemical parameters to achieve the maximum possible removal efficiencies. Further, an ANalysis Of VARiance (ANOVA) model was adopted to investigate the reliability of the developed empirical model.

RESULTS AND DISCUSSIONS

Physical characterization:

The adsorbents NACSAA and NACSAB were characterized for various textual properties and the obtained results are depicted in Table 1. BET surface area for NACSAA and NACSAB (before after adsorption of MGD) was measured and the obtained values are noted in Table 1.

Surface characterization:

Field emission scanning electron microscope (FESEM)

The SEM monographs were taken for the adsorbents: NACSAA and NACSAB (before and after MGD loading) and are presented in Figure 3(a)–3(d). These SEM monographs reveal the porosity and surface texture of the samples. Figure 3 shows the SEM monographs of NACSAA and NACSAB before and after MGD loading. It is clearly seen from Figure 3(a) and 3(b) that the surfaces of the adsorbents

Table 1 | Textual properties of the adsorbents NACSAA and NACSAB

S. No.	Physical parameter	NACSAA	NACSAB
	Apparent density (g/mL)	0.52	0.38
	Moisture content (%)	5.07	5.68
	Ash content (%)	3.42	3.22
	Iodine number (mg/g)	621	634
	Particle size (μ)	75	75
	BET surface area (mm^2/g)		
	Before adsorption	320.54	342.42
	After adsorption	285.22	272.54
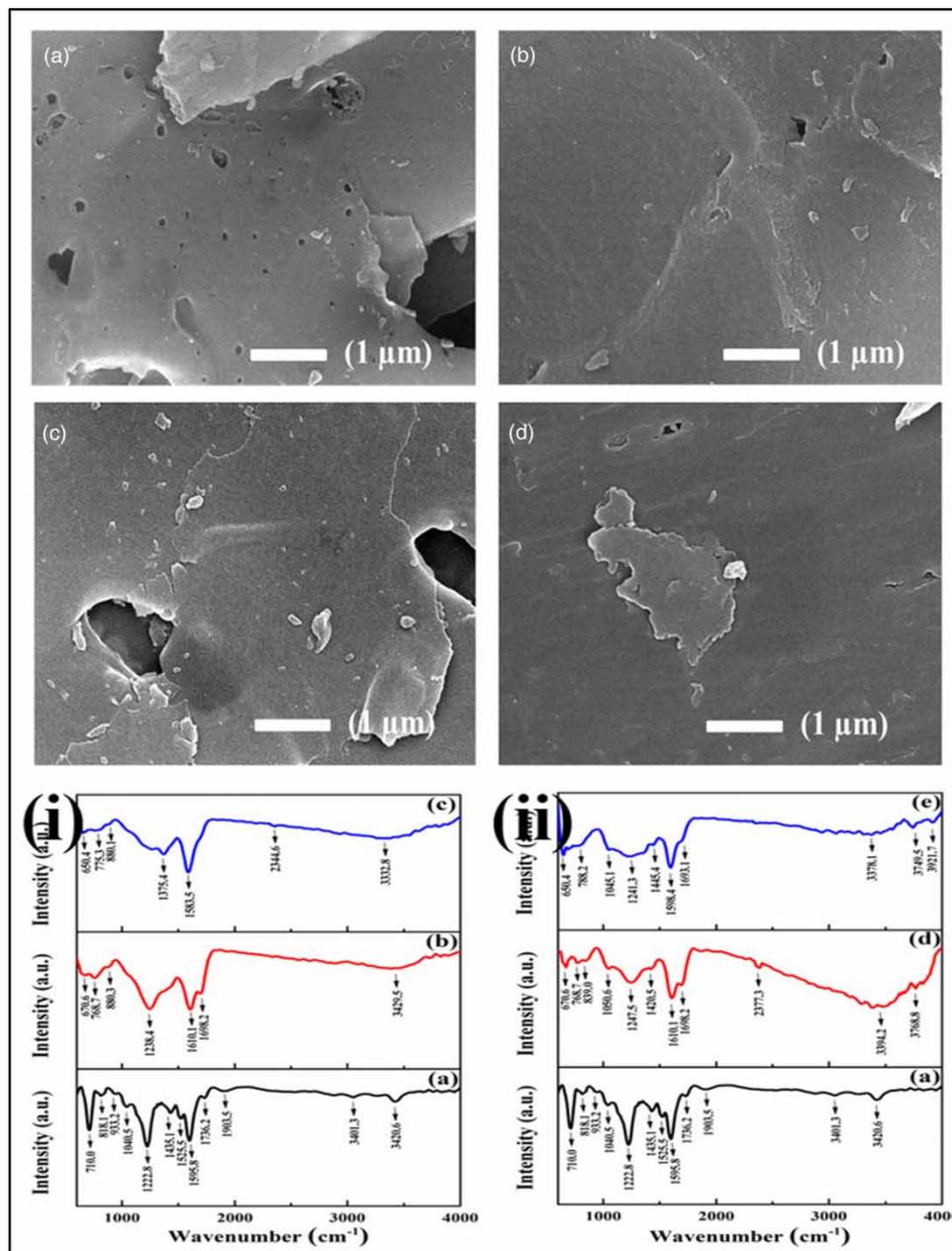
Figure 3 | SEM images of (a) NACSAA (before); (b) NACSAA (after); (c) NACSAB (before); (d) NACSAB (after) loading of MGD; FT-IR spectra of (i): (a) MGD, (b) NACSAA (before), (c) NACSAA (after) (ii): (a) MGD, (d) NACSAB (before), (e) NACSAB (after) loading of MGD.

are rough and uneven in nature and have considerably porous textures, which are requisite for the effective adsorption of MGD. The surfaces of the adsorbents (Figure 3(c) and 3(d)) are smooth and homogeneous in nature and the pores are completely clogged after adsorption of MGD. These results confirm the sorption of MG dye onto the surface of both the adsorbents.

FT-IR

Figure 3(i) and 3(ii) represent the FT-IR spectra of MGD, NACSAA and NACSAB before and after MGD loading.

MGD.   On perusal of the FT-IR spectrum of MGD, the ten significant peaks, such as two peaks at 710 cm^{-1} and 818 cm^{-1} pertaining to bending vibrations of the C–H group; the peak at 1,040 cm^{-1} corresponding to the -C-O group; the band at 1,222 cm^{-1} corresponding to C-N stretching vibrations; the band at 1,435 cm^{-1} pertaining to –C-H- deformations in alkanes; the peaks at 1,525 cm^{-1} and 1,595 cm^{-1} corresponding to C$=$C stretching of the benzene ring; the band at 1,736 cm^{-1} pertaining to the –C$=$O group and two bands at 3,401 cm^{-1} and 3,420 cm^{-1} pertaining to stretching vibrations of the N–H group in primary amines are noticed.

NACSAA.   On comparing the spectra of NACSAA before and MGD after adsorption, it is observed that the band at 1,238 cm^{-1} (before adsorption) pertaining to C-N stretching vibrations is shifted to 1,375 cm^{-1} (after) and the intensity of this band is decreased. **The peak at 1,583 cm^{-1} corresponding to C$=$C stretching of the benzene ring appeared in the spectrum after adsorption of MGD.** Moreover, the intensity of the peak representing the stretching vibration of the O–H group is decreased and the absorption peak is shifted from 3,429 cm^{-1} to 3,332 cm^{-1} after MGD loading. The shifting and appearance of new peaks may be attributed to the fact that there are interactions between the adsorbate MGD and the adsorbent.

NACSAB.   On perusal of spectra of NACSAB (before and after MGD loading), it is noted that the band pertaining to C–H bending vibrations at 670 cm^{-1} (before) is shifted to 650 cm^{-1} (after); 768 cm^{-1} (before) shifted to 788 cm^{-1} (after); a band at 1,050 cm^{-1} (before) pertaining to the –C-O- group is shifted to 1,045 cm^{-1} (after); a peak at 1,420 cm^{-1} (before) corresponding to –C-H- deformations in the alkanes is shifted to 1,445 cm^{-1}. A new band at 1,598 cm^{-1} pertaining to C$=$C stretching of the benzene ring appeared in the spectrum after adsorption of MGD. The peak at 1,698 cm^{-1} (before) pertaining to the –C$=$O group is shifted to 1,693 cm^{-1} (after); Further, the strength of the peak representing the stretching vibration of the O–H group is decreased and the absorption peak is shifted from 3,394 cm^{-1} to 3,378 cm^{-1} after adsorption of MGD. These changes indicate that MGD adsorption has taken place via surface interactions and molecular adsorption into the pores of the adsorbents by capillary forces.

Influence of combined effect of adsorption parameters of MGD on to NACSAA and NACSAB

The analysis of the combined effect of physicochemical parameters for the extraction of MGD on to the adsorbents NACSAA and NACSAB was carried out and the findings are presented in Figures 4(a), 4(b), 5(a)–5(f) and 6(a)–6(f).

Figures 5(a), 5(b), 6(a) and 6(b) represent the combined influence of pH with sorbent dosage and contact time respectively on extraction of MGD ions for the adsorbents NACSAA and NACSAB. The influence of pH on the removal ability of the adsorbents was examined by changing the pH from 2 to 10, keeping constant the other parameters of extraction. It is seen from the figures that the percentage of extraction of MGD increases with increase in pH and the extraction is most

favorable at basic pH 8–9 with 91% and 100% extraction of MGD onto NACSAA and NACSAB respectively. This can be explained from the pHzpc values which are found to be 5.0 for NACSAA and 5.53 for NACSAB as described in Figure 4(a) and 4(b).
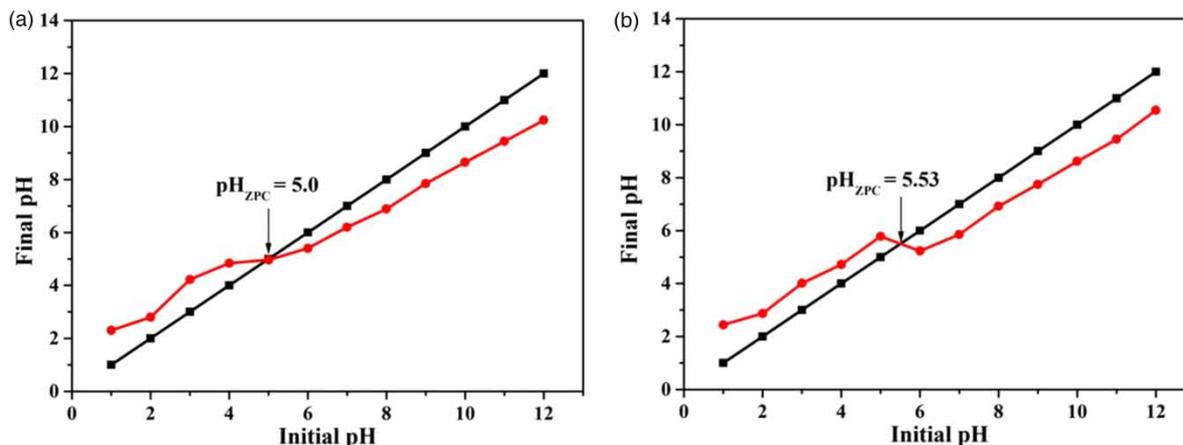

Figure 4 | Determination of pHzpc: (a) NACSAA (b) NACSAB.

At pH < pHzpc, the % removal of dye is less because of the protonation of the adsorbents' surface, which obstructs the extraction of MGD ions. But when the solution pH > pHzpc, the surface of the adsorbents becomes deprotonated and at high pH values, the surface acquires negative charge. Thus the acquired negative charge imparts a kind of a thrust on the inter-surface of the adsorbent and solution for positive ions. Hence, the MGD being a cation below pH: ~10.5 (pK–10.3), shows more adsorption towards the adsorbents in the pH range 8–9 because the ideal conditions for adsorption are that the dye is in the cationic form and the surface must have a negative charge; these conditions are satisfied in the said pH range. But when the solution pH is further increased, the dye species are hydrolyzed in basic conditions which leads to the loss of the positive surface charge and so the percentage of extraction is less favored at high pH values.

Figures 5(c) and 6(c) represent the combined influence of initial concentration with pH for the extraction of MGD ions on to the adsorbents NACSAA and NACSAB. The influence of the initial MGD concentration on the rate of adsorption was investigated by changing the initial dye concentration in the range of 100–500 mg/L. From the figures it is observed that, with rise in the initial MGD concentration, the % removal of MGD decreased from 91% to 48% with the adsorbent NACSAA and 100% to 53% with NACSAB. This is attributed to the fact that, at low MGD concentrations, the ratio of the number of adsorbate ions to the available sorption sites of the adsorbents is fewer. Hence, the adsorption is independent of the initial concentration of dye resulting in more % removal. But as the initial concentration increases, the available sites become far less and so the extraction of MGD is dependent on the initial dye concentration (Saha *et al.* 2010a) and hence, the % removal is less.

But, the adsorption ability (q_e) is enhanced from 15.16 to 40.0 mg/g for NACSAA and with NACSAB it is increased from 20.0 to 53.0 mg/g. This is because, with a rise in the initial dye concentration, the dye molecules are induced to correlate with the active sorption sites of the adsorbents and hence, the uptake of dye by the adsorbents is increased.

Figures 5(d), 5(e), 6(d) and 6(e) represent the combined influence of adsorbent dosage with contact time and initial concentration respectively on the adsorption of MGD ions onto the adsorbents NACSAA and NACSAB respectively. The influence of sorbent dosage on the removal efficiency of the adsorbents was investigated by changing the adsorbents' dosage from 0.2 g/100 mL to 1.0 g/100 mL while keeping constant the other parameters of adsorption. It is noted from the figure that with increase in adsorbent dosage, the % removal is enhanced and 91% (maximum) of
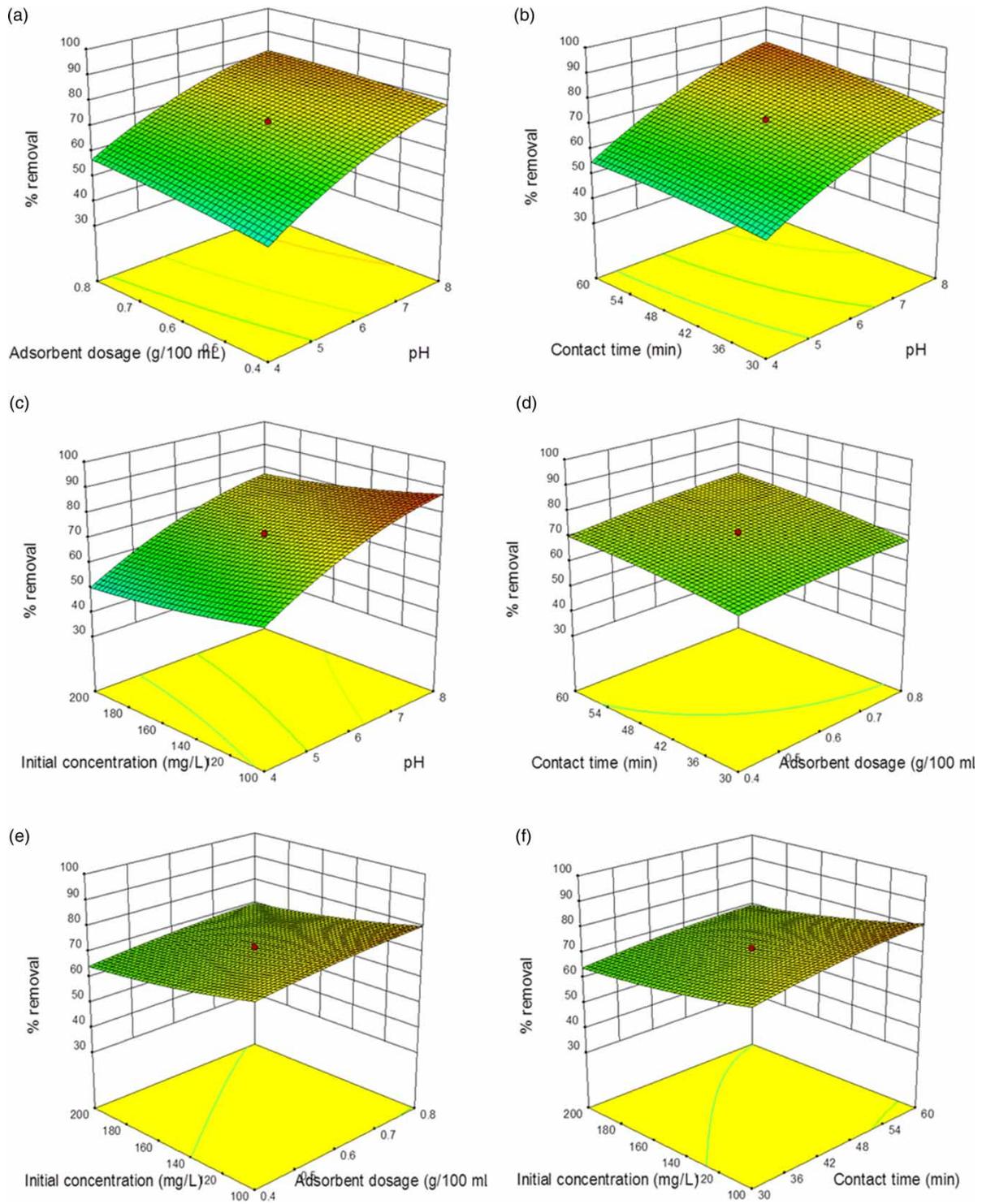
Figure 5 | Combined effects of physicochemical parameters of MBD on to NACSAA.

extraction is noted with 0.6 g/100 mL of NACSAA and 100% extraction of MGD is observed with 0.5 g/100 mL of NACSAB. Thereafter, the % removal decreased slightly with increase in the sorbent dosage, which is attributed to the fact of aggregation of active sorption sites. This results in a decrease in the existing surface area to MGD for adsorption and hence, less percentage removal.

Figures 5(f) and 6(f) represent the combined influence of contact time and initial concentration on extraction of MGD onto the adsorbents NACSAA and NACSAB respectively. The influence of contact time on the extraction ability of the adsorbents was studied by changing the contact time
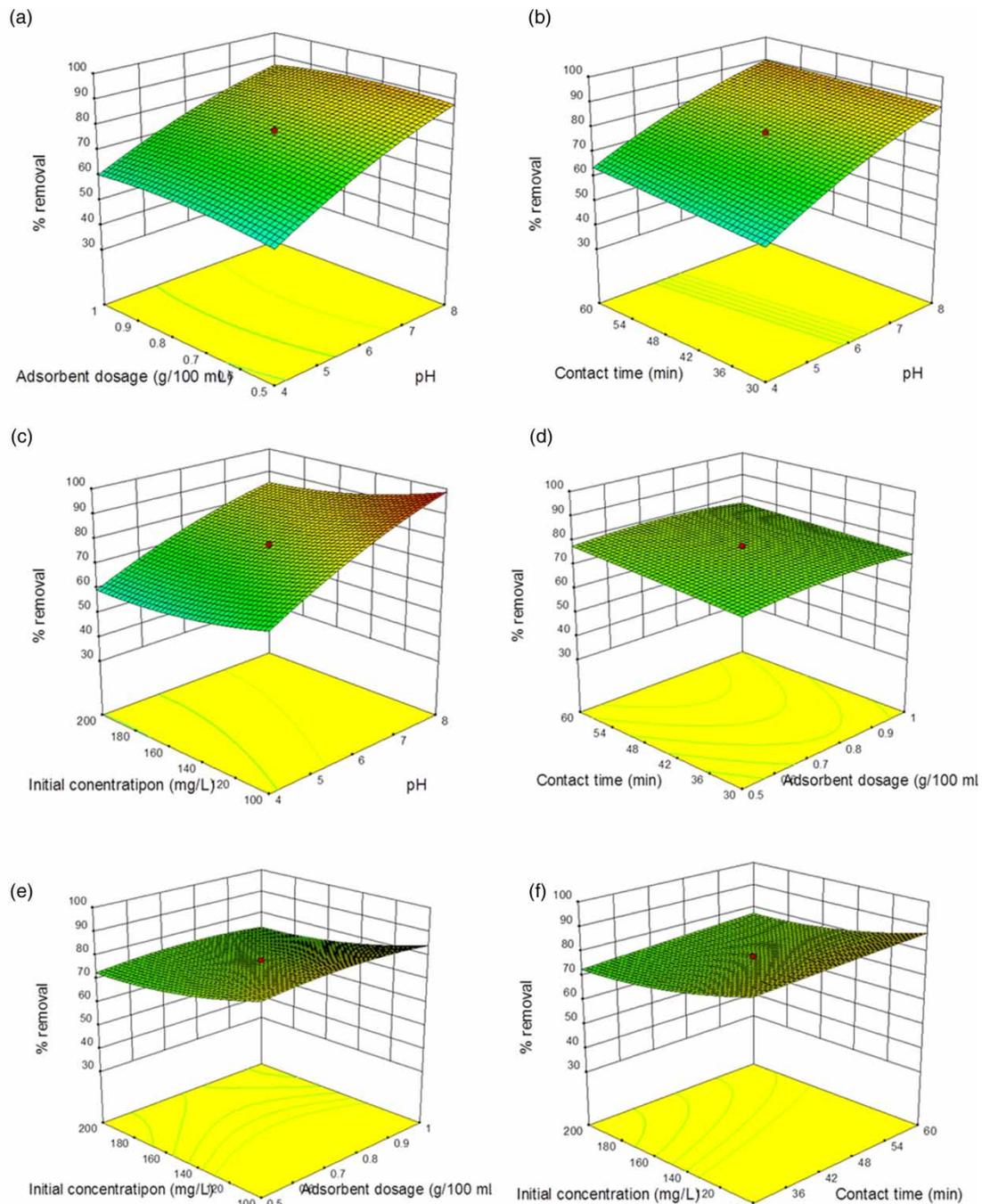
Figure 6 | Combined effects of physicochemical parameters of MBD on to NACSAB.

from 15 minutes to 75 minutes while keeping constant the other parameters of adsorption. It is noted from the figure that the adsorption of MGD is enhanced with the rise in contact time and reached the maximum percentage of extraction of 91% with NACSAA and 100% with NACSAB after 50 minutes and 40 minutes of agitation respectively and further increase of time of contact did not enhance the removal efficiency of MGD as all the active sites are utilized with time till a steady state is reached. The adsorption process occurred rapidly in the initial stages because of the large obtainability of sorption sites of the adsorbents, and in the advanced stages, the number of active sites were scarcely available. Hence, the extraction process becomes attachment-controlled and the process of extraction slows down.

Moreover, the plots of actual values vs. predicted values for the extraction of MGD onto the adsorbents NACSAA and NACSAB respectively are shown in Figure S1. It is observed from the figures that, the actual values and the expected values are in agreement with one another, as has been revealed from the good correlation coefficient values (R^2) for the adsorbents NACSAA (0.9872) and NACSAB (0.9683). The statistical values obtained from the ANOVA model for the adsorption of MGD are presented in Figures S2 and S3.

The optimum conditions of extraction for the adsorbent NACSAA are found to be: pH: 8–9; sorbent dosage: 0.6 g/100 mL; contact time: 45 minutes; initial MGD concentration: 50 mg/L and temperature: 30 °C $\pm$ 1 °C.

% removal (Y) with NACSAA: $-9.55000 + 18.70000 * A + 42.00000 * B + 0.36333 * C - 0.22633 * D - 2.42187 * AB + 0.051042 * AC + 3.12500E\text{-}004 * AD + 0.18958 * BC + 6.87500E\text{-}003 * BD - 9.08333E\text{-}004 * CD - 1.07266 * A^2 - 19.76563 * B^2 - 4.62500E\text{-}003 * C^2 + 5.28750E\text{-}004 * D^2 = 91.0\%$

The optimum conditions of extraction for the adsorbent NACSAB were found to be: pH: 8–9; sorbent dosage: 0.5 g/100 mL; contact time: 30 minutes; initial MGD concentration: 50 mg/L and temperature: 30 °C $\pm$ 1 °C.

% removal (Y) with NACSAB $= +78.00 + 14.05 * A + 0.31 * B + 1.89 * C - 5.43 * D - 1.21 * AB - 1.09 * AC - 1.22* AD - 0.54 * BC - 0.025 * BD + 0.35 * CD - 2.77 * A^2 - 2.10 * B^2 - 0.10 * C^2 + 2.77 * D^2 = 100.0\%$.

Thermodynamic studies:

Thermodynamic parameters (ΔH, ΔS and ΔG) were assessed by changing the temperature from 303 k to 333 k by keeping constant the other adsorption parameters. The observations are as shown in Figure 7(a) and 7(b). For this study, $\ln K_d$ was plotted against $1/T$ as per the Van't Hoff Equation: $\ln K_d = \Delta S/R - \Delta H/RT$, where $K_d = q_e/C_e$ and from which ΔH and ΔS are calculated; the ΔG value was calculated from the relation $\Delta G = \Delta H - T\Delta S$, where K_d (L/mg) is the distribution coefficient for the adsorption, q_e is the amount of dye adsorbed on the adsorbent at equilibrium, C_e is the equilibrium concentration of the dye in the solution, T is the absolute temperature, and R is the gas constant (Romero-Gonzalez *et al.* 2005). K_d values in L/mg were converted into L/g by multiplication with a factor of 1,000 and the values acquired were multiplied with the m. wt. (molecular weight) of the MGD to convert the units of K_d to L/mol (Lima *et al.* 2015).

The values of different thermodynamic parameters are tabulated in Table 2. It is noted from the table that the positive value of ΔH reflects the endothermic nature of the adsorption process and that fact is supported by the increase in K_d values with rise in temperature. ΔS values are positive and they demonstrate the affinity between the adsorbents and MDG. Moreover, the ΔG values are negative, indicating the spontaneity of adsorption.

Influence of co-ions on MGD removal:

The influence of co-anions, namely NO_3^-, Cl^-, CO_3^{2-}, SO_4^{2-} and PO_4^{3-} and co-cations; that is, Na^+, Zn^{2+}, Mg^{2+}, Ca^{2+}, and Cu^{2+} are naturally present in water and these ions strive with the MGD molecules for the active vacant sites of adsorption and subsequent decrease in the removal efficiencies of adsorbents results. The influence of competing ions on the extraction ability of dye was investigated using 500 mg/L concentrations of co-ions and an initial dye concentration of 100 mg/L, keeping constant the other adsorption parameters: pH: 8; agitation time: 50 min for NACSAA, 40 min for NACSAB; sorbent concentration: 0.6 g/100 mL for NACSAA, 0.5 g/100 mL for NACSAB and temperature 30 °C $\pm$ 1 °C. The data obtained is depicted in Figure 7(c) and 7(d). It is observed from the figure that the percentage extractability of MGD is slightly influenced by the anions but cations have some effect. The interference of cations on the % of extraction of MGD is in the order: $Zn^{2+} > Ca^{2+} > Mg^{2+} > Cu^{2+} > Na^+$.
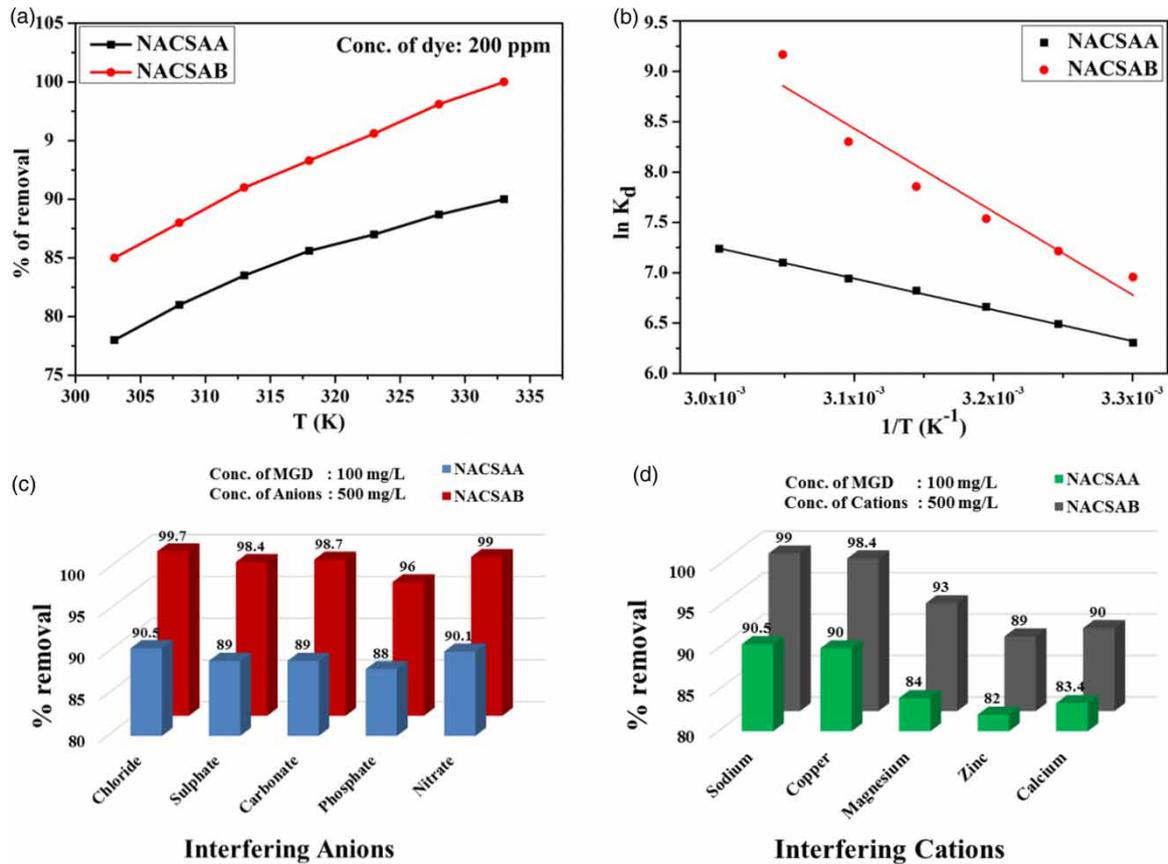
Figure 7 | Influence of temperature and interfering ions on the extraction of MGD. (a) T vs. % removal; (b) 1/T vs. ln K_d; (c) interfering anions; (d) interfering cations.

Table 2 | Thermodynamic parameters of adsorption of MGD on to NACSAA & NACSAB

Type of adsorbent	ΔH kJ/mol)	ΔS (J/mol)	ΔG (kJ/mol)							R²
			303 K	308 K	313 K	318 K	323 K	328 K	333 K	
NACSAA	25.76	137.59	−15.92	−16.61	−17.30	−17.99	−18.67	−19.36	−20.05	0.99
NACSAB	68.69	283.009	−17.05	−18.47	−19.88	−21.30	−22.71	−24.13	−25.54	0.91

Adsorption isotherms:

Freundlich, Langmuir, Dubinin-Radushkevich and Temkin (Freundlich 1906; Langmuir 1918; Temkin & Pyzhev 1940; Dubinin & Radushkevich 1947) are the four well-known models of adsorption isotherms used to determine the adsorption abilities of adsorbents for the extraction of dye. The linear forms of Freundlich, Langmuir, Dubinin-Radushkevich and Temkin respectively are given in Equations (1)–(4).

$$ln q_e = -\beta\varepsilon^2 + ln q_m \tag{1}$$

$$\frac{C_e}{q_e} = \left(\frac{a_L}{k_L}\right)C_e + \frac{1}{k_L} \tag{2}$$

$$q_e = B\, ln C_e + B\, ln A \tag{3}$$

$$log\, q_e = log\, k_F + \left(\frac{1}{n}\right)log\, C_e \tag{4}$$

where C_e (mg/L) is the equilibrium MGD concentration in the solution, q_e (mg/g) is the amount of MGD sorbed onto the surface of adsorbents, K_F and $1/n$ are the constants of Freundlich isotherm, K_L (L/mg) and a_L are the Langmuir equilibrium constants, q_m is the amount of adsorbate required to form a monolayer (mg/g). A and B are Temkin constants, where $B = RT/b$, $\varepsilon = RT \ln(1 + 1/C_e)$, $E = 1/\sqrt{2\beta}$, $\beta =$ a constant of energy, $R =$ gas constant and $T =$ absolute temperature and the corresponding plots are shown in Figure 8(a)–8(d) and the values obtained are presented in the Tables 3 and 4.

R_L is a dimensionless separation factor obtained from the Langmuir model, R_L is described using $R_L = 1/(1 + a_L C_i)$. The R_L values for the adsorbents NACSAA and NACSAB are 0.00986 and 0.00988 respectively, as the R_L values are less than 1, the adsorption process is favorable (Atkins 1999; Monika *et al.* 2009).

The R^2 values from the Table 3 indicate that the process of extraction is explained in the following decreasing order: Freundlich model > Langmuir > Temkin > Dubinin-Radushkevich for both the adsorbents. The well fitted model is Freundlich representing the heterogeneity of the adsorbents surface and multi-layered process of adsorption.

Adsorption kinetics:

The mechanism of adsorption of MGD onto the adsorbents is elucidated by employing different models of kinetics namely, pseudo first-order, pseudo second-order (Ho & McKay 1999; Ho *et al.* 2000), Elovich and Bangham's pore diffusion models and the linear forms of the said kinetic models are expressed in the Equations (5)–(8) as follows.

$$log\,(q_e - q_t) = \, log\,q_e - \frac{k_1 t}{2.303} \tag{5}$$

$$\frac{t}{q_t} = \frac{1}{k_2 q_e^2} - \left(\frac{1}{q_e}\right)t \tag{6}$$

$$q_t = \frac{1}{\beta}ln(\alpha\beta) + \frac{1}{\beta}\,ln\,t \tag{7}$$

$$log\left[log\left(\frac{C_i}{C_i - q_t m}\right)\right] = log\frac{k_0}{2.303\,V} + \alpha\,logt \tag{8}$$

where q_e and q_t (mg/g) are amounts of MGD adsorbed onto the adsorbents at equilibrium and after time 't', respectively. k_1 (min^{-1}) and k_2 (g/mg.min) are the rate constants of the pseudo first-order and pseudo second-order models respectively. β is the desorption constant and α is the initial MGD sorption rate (mmol.(g min)$^{-1}$), the corresponding plots are presented in Figure 8(e)–8(h).

R^2 values and the rate constants of the described kinetic models are measured and depicted in Tables 3 and 4 respectively. It is revealed from the table that the R^2 value is high for the pseudo-second order model for both the adsorbents: 0.994 for NACSAA and 0.995 for NACSAB. This infers the pseudo-second-ordered adsorption kinetics for both adsorbents.

Desorption, regeneration and reuse

Desorption experiments were made using the procedure as described in previous literature (Sujitha & Ravindhranath 2018c). It is observed that 0.1 M HCl was effective. Figure 9 shows the performance of regenerated adsorbents in the removal of MGD as % removal vs. No. of cycles. It is observed from the figure that the removal efficiency is more than 80.0% for every cycle and it did not come down below 80.0% even after five regenerations for both the adsorbents. Thus, it can be deduced that the adsorbents can be used repeatedly in the treatment of wastewater containing dyes.
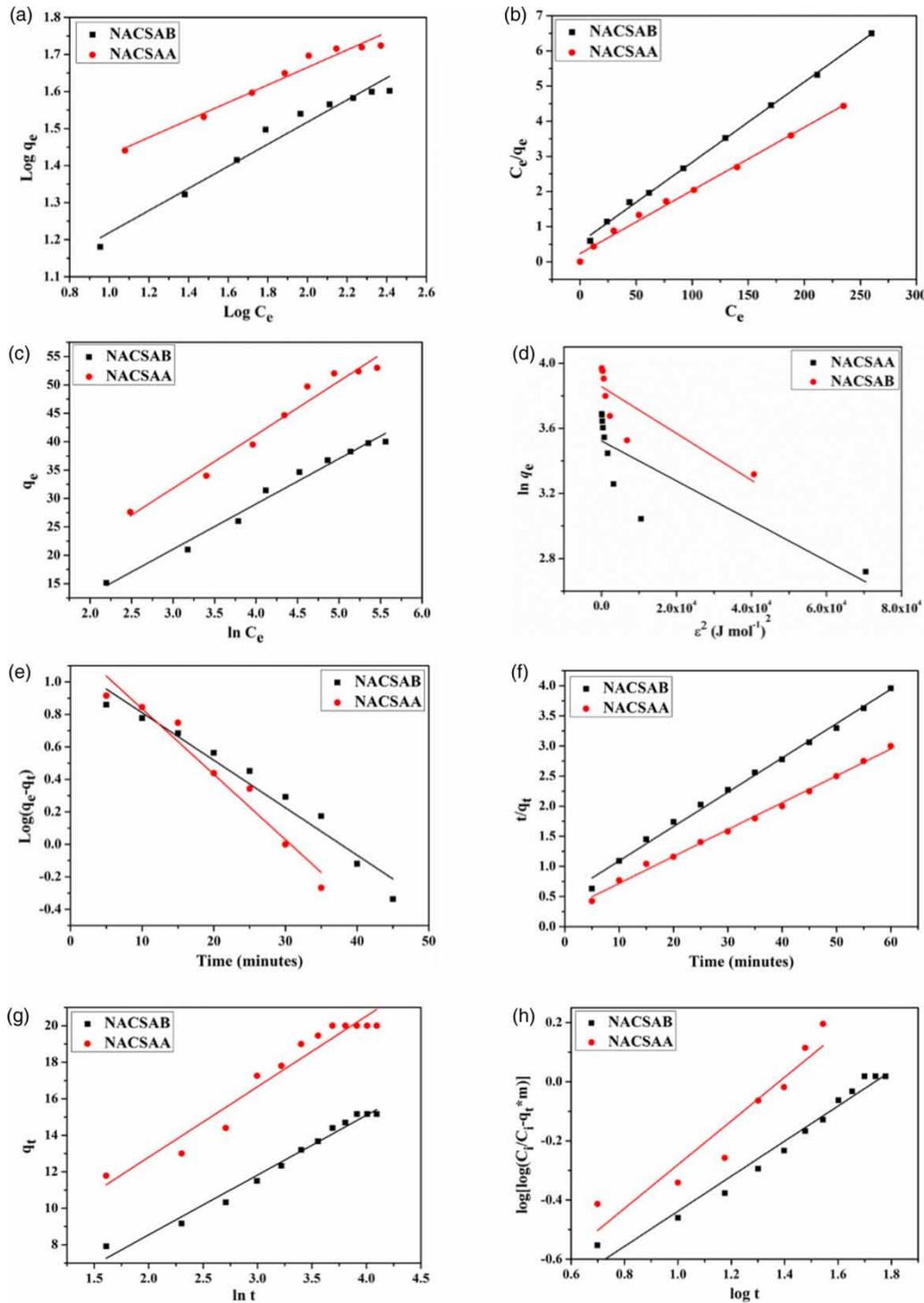
Figure 8 | Adsorption isotherm models: (a) Langmuir (b) Freundlich (c) Tempkin (d) Dubinin-Radushkevich; various models of adsorption kinetics: (e) pseudo-first order, (f) pseudo-second order, (g) Elovich, (h) Bangham's pore diffusion.

Applications

The developed NACSAA and NACSAB-based methodologies were applied to the effluent samples obtained from different dyeing industries in A.P. (Andhra Pradesh) and the observations are noted in Table 5. Not less than 80.0% extraction of MGD was observed with these effluent samples.

Table 3 | Adsorption and kinetic parameters for NACSAA and NACSAB*

| Adsorbent | | Adsorption isotherms | | | | Kinetic models | | | |
		Langmuir	Freundlich	Dubinin-Radushkevich	Temkin	Pseudo- first order	Pseudo-second order	Elovich	Bangham's pore diffusion
NACSAA	m	0.298	0.0228	−1.229E-05	7.971	−0.0292	0.0569	3.275	0.592
	C	0.920	0.550	3.523	−2.85	1.102	0.522	1.996	−1.03
	R^2	0.962	0.998	0.673	0.979	0.956	0.994	0.978	0.97
NACSAB	m	0.236	0.0179	−1.438E-05	9.423	−0.04	0.0446	3.864	0.738
	C	1.19	0.234	3.856	3.524	1.237	0.272	5.068	−1.019
	R^2	0.963	0.992	0.658	0.964	0.948	0.995	0.937	0.882

*m = slope, C = intercept, R^2 = correlation coefficient.

Table 4 | Adsorption and kinetic parameters of adsorbents NACSAA and NACSAB

Adsorption isotherms	Parameters	NACSAA	NACSAB
Langmuir	K_L (L/mg)	1.0869	0.840
	a_L	0.323	0.198
Freundlich	K_F (L/mg)	13.64	8.77
Temkin	B (J/mol)	7.971	9.423
Dubinin-Radushkevich	β	−1.229E-05	−1.438E-05
	E (kJ/mol)	0.2017	0.1864
Kinetics models	**Rate constants**	**NACSAA**	**NACSAB**
Pseudo-first order	K_1 (min^{-1})	0.0672	0.0921
Pseudo-second order	K_2 (g/mg min)	0.00613	0.00731
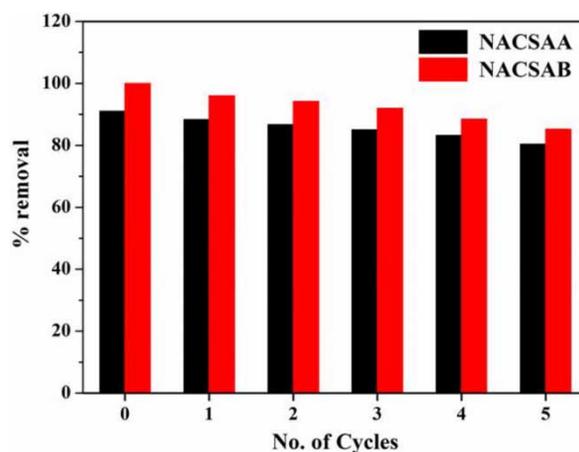
Figure 9 | Number of regenerations vs. % removal.

Investigation of MGD adsorption ability (q_e) in comparison with the reported adsorbents

The NACSAA and NACSAB-based methods developed in this investigation were compared with the reported literature (Zhang *et al.* 2008; Arivoli *et al.* 2009; Khattri & Singh 2009; Sekhar *et al.* 2009; Saha *et al.* 2010b; Tsai & Chen 2010; Parthasarathy *et al.* 2011; Santhi *et al.* 2011; Chieng *et al.* 2014; Gautam *et al.* 2015; Mirzajani & Ahmadi 2015) with respect to q_e (mg/g) and pH (Table 6). It is inferred from the table that NACSAA (40.0 mg/g) and NACSAB (53.0 mg/g) have shown higher adsorption capacity than hitherto reported adsorbents in the literature.

Table 5 | Applications: MGD adsorption from the effluent samples obtained from different dyeing industries of A.P.* (pH: 8; sorbent concentration: 0.6 g/100 mL for NACSAA, 0.5 g/100 mL for NACSAB; contact time: 50 min for NACSAA, 40 min for NACSAB and temperature 30 °C $\pm$ 1 °C)

S. No.	Samples collected from various dyeing industries in Andhra Pradesh	C_i (mg/L) initial conc. of MGD in the sample	NACSAA		NACSAB	
			C_e (mg/L)	% removal	C_e (mg/L)	% removal
1	Sample 1	90	1.8	98	0	100
2	Sample 2	115	12.65	89	1.49	98.7
3	Sample 3	125	16.5	86.8	6.0	95.2
4	Sample 4	150	23.4	84.4	10.8	92.8
5	Sample 5	168	29.4	82.5	16.63	90.1
6	Sample 6	180	34.74	80.7	22.5	87.5

*C_e: equilibrium concentration of MGD in the sample.
*The values are the average of five determinations; SD $= \pm 0.67$.

Table 6 | Investigation of MGD adsorption ability (q_e) in comparison with the reported adsorbents

S. No	Adsorbent	pH	q_e (mg/g)	Reference
1.	Tamarind fruit shell	5.0	1.95	Saha et al. (2010b)
2.	A.squamosa seeds	6.0	25.9	Santhi et al. (2011)
3.	Fe-Zn nano particles	9.0	21.7	Gautam et al. (2015)
4.	Carbon prepared from Arundo donax root	5–7	8.69	Zhang et al. (2008)
5.	Melamine supported Fe_3O_4 nano particles	6.5	9.1	Mirzajani & Ahmadi (2015)
6.	Peat	7.0	15.3	Chieng et al. (2014)
7.	Carbon prepared from Borassus bark	6	20.70	Arivoli et al. (2009)
8.	Neem sawdust	7.2	4.35	Khattri & Singh (2009)
9.	Dried cashew nut bark carbon	6.60	20.09	Parthasarathy et al. (2011)
10.	Cellulose powder	7.0	2.422	Sekhar et al. (2009)
11.	Chlorella-based biomass	7.0	18.4	Tsai & Chen (2010)
12	NACSAA	8.0	40.0	Present study
13.	NACSAB	8.0	53.0	Present work

CONCLUSIONS

Two adsorbents were developed based on HNO_3 activated carbons from stems of *Achyranthes aspera* and *Allamanda blanchetii* plants; namely, NACSAA and NACSAB. These bio-adsorbents were probed for the extraction of cationic malachite green dye from contaminated water by varying the extraction conditions for the maximum possible extraction.

The adsorbents were characterized by various surface morphological techniques including FESEM and FT-IR. The adsorption abilities were found to be 40.0 mg/g for NACSAA and 53.0 mg/g for NACSAB respectively, and these figures are higher than many sorbents reported in literature.

The percentage extractability of MGD was slightly affected by the anions but cations had some effect. The interference of cations on the % of extraction of MGD was in the order: $Zn^{2+} > Ca^{2+} > Mg^{2+} > Cu^{2+} > Na^+$.

The mechanism of adsorption was assessed by different adsorption isotherm models and is explained in the following decreasing order: Freundlich model > Langmuir > Temkin > Dubinin-Radushkevich for both the adsorbents. The best fit model is Freundlich, representing the heterogeneous nature of the surfaces of sorbents and a multi-layer process of extraction.

Of the different kinetic models investigated, the adsorption is well described by pseudo-second ordered kinetics. Thermodynamics parameters (ΔG, ΔS and ΔH) reveal the endothermic and spontaneous process of sorption for both the adsorbents. The fall in ΔG values with the rise in temperature demonstrates the favorable extraction conditions at high temperatures.

Substantial amounts of dye (not less than 80.0%) are noted even with five time regenerated spent adsorbents, NACSAA and NACSAB. The procedures developed in this investigation were successfully applied to water samples procured from different dyeing industries.

ACKNOWLEDGEMENT

REFERENCES

Aksakal, O., Ucun, H. & Kaya, Y. 2009 Application of *Eriobotrya japonica* (Thunb) Lindley (Loquat) seed biomass as a new biosorbent for the removal of malachite green from aqueous solution. *Water Sci. Technol.* **59**, 1631–1639.

American Public Health Association (APHA) 1998 *Standard Methods for the Examination of Water and Waste Water*, 20th edn. American Public Health Association, Washington, DC, USA.

Arivoli, S., Hema, M., Martin, P. & Prasath, D. 2009 Adsorption of malachite green onto carbon prepared from borassus bark. *Arab. J. Sci. Eng.* **34**(2), 31.

Arrellano-Cárdenas, S., Lopez-Cortez, S., Cornejo-Mazon, M. & Mares-Gutierrez, J. 2013 Study of malachite green adsorption by organically modified clay using a batch method. *Appl. Surf. Sci.* **280**, 74–78.

Ashtoukhy, E. I. S. Z. E. I. 2009 Loofa egyptiaca as a novel adsorbent for removal of direct blue dye from aqueous solution. *J. Environ. Manage.* **90**, 2755.

ASTM D4607 – 14 2014 *Standard Test Method for Determination of Iodine Number of Activated Carbon*. ASTM International, West Conshohocken, PA, USA.

Atkins, P. 1999 *Physical Chemistry*, 6th edn. Oxford University Press, London, UK, pp. 857–864.

Banerjee, S., Sharma, G. C., Gautam, R. K., Chattopadhyaya, M. C., Upadhyay, S. N. & Sharma, Y. C. 2016 Removal of Malachite Green, a hazardous dye from aqueous solutions using *Avena sativa* (oat) hull as a potential adsorbent. *J. Mol. Liq.* **213**, 162–172.

BIS (Bureau of Indian Standards) 1989 *Activated Carbon Powdered and Granular-Methods of Sampling and its Tests*. BIS, New Delhi, India, pp. 877.

Box, G. E. P. & Hunter, J. S. 1957 Multi-factor experimental designs for exploring response surfaces. *Ann. Math. Stat.* **28**, 195–241.

Brunauer, S., Emmett, P. H. & Teller, E. 1938 Adsorption of gases in multimolecular layers. *J. Am. Chem. Soc.* **60**(2), 309–319.

Chieng, H. I., Zehra, T., Lim, L. B. L., Priyantha, N. & Tennakoon, D. T. B. 2014 Sorption characteristics of peat of Brunei Darussalam IV: equilibrium, thermodynamics and kinetics of adsorption of methylene blue and malachite green dyes from aqueous solution. *Environ. Earth Sci.* **72**, 2263–2277.

Dubinin, M. M. & Radushkevich, L. V. 1947 The equation of the characteristic curve of the activated charcoal. *Proc. Acad. Sci. Phys. Chem. Sect.* **55**, 331–333.

Freundlich, H. M. F. 1906 Over the adsorption in solution. *J. Phys. Chem.* **57**, 385–471.

Gautam, R. K., Banerjee, V. R. S., Sanroman, M. A. & Singh, S. S. K. 2015 Synthesis of bimetallic Fe–Zn nanoparticles and its application towards adsorptive removal of carcinogenic dye malachite green and Congo red in water. *J. Mol. Liq.* **232**, 227–236.

Gupta, N., Kushwaha, A. K. & Chattopadhyaya, M. C. 2011 Application of potato (Solanum tuberosum) plant wastes for the removal of methylene blue and malachite green dye from aqueous solution. *Arabian J. Chem.* **9**, S707–S716.

Ho, Y. S. & McKay, G. 1999 Pseudo-second order model for sorption processes. *Process Bio Chem.* **34**, 451–465.

Ho, Y. S., Ng, J. C. Y. & McKay, G. 2000 Kinetics of pollutant sorption by bio sorbents: a review. *Sep. Purif. Reviews* **29**(2), 189–232.

Jerold, M. & Sivasubramanian, V. 2016 Biosorption of malachite green from aqueous solution using brown marine macro algae *Sargassum swartzii*. *Desalin. Water Treat.* **57**, 25288–25300.

Khattri, S. D. & Singh, M. K. 2009 Removal of malachite green from dye wastewater using neem sawdust by adsorption. *J. Hazard. Mater.* **167**, 1089.

Langmuir 1918 The adsorption of gases on plane surfaces of glass, mica and platinum. *J. Am. Chem. Soc.* **40**, 1361–1368.

Lim, L. B. L., Priyantha, N. & Mohd Mansor, N. H. 2016 Utilizing *Artocarpus altilis* (breadfruit) skin for the removal of malachite green: isotherm, kinetics, regeneration, and column studies. *Desalin. Water Treat.* **57**, 16601–16610.

Lima, E. C., Adebayo, M. A. & Machado, F. M. 2015 Chapter 3- Kinetic and equilibrium models of adsorption in carbon nanomaterials as adsorbents for environmental and biological applications. ISBN 978-3-319-18874-4, Springer, Dordrecht, the Netherlands, 33-69.

Mirzajani, R. & Ahmadi, S. 2015 Melamine supported magnetic iron oxide nanoparticles (Fe_3O_4@Mel) for spectrophotometric determination of malachite green in water samples and fish tissues. *J. Ind. Eng. Chem.* **23**, 171–178.

Mohammad, R., Rajoo, A. T. & Mohamad, M. 2017 Coconut fronds as adsorbent in the removal of malachite green dye. *J. Eng. Appl. Sci.* **12**, 996–1001.

Mohd Azmier Ahmad, M. A., Ahmad, N. & Bello, O. S. 2014 Adsorptive removal of malachite green dye using durian seed-based activated carbon. *Water, Air, Soil Pollut.* **225**, 2057.

Monika, J., Garg, V. & Kadirvelu, K. 2009 Chromium (VI) removal from aqueous solution using sunflower stem waste. *J. Hazard. Mater.* **162**, 365–372.

Naga Babu, A., Krishna Mohan, G. V., Kalpana, K. & Ravindhranath, K. 2018 Removal of fluoride from water using H_2O_2-treated fine red mud doped in Zn-alginate beads as adsorbent. *J. Environ. Chem. Eng.* **6**, 906–916.

Namasivayam, C. & Kadirvelu, K. 1997 Agricultural solid wastes for the removal of heavy metals: adsorption of Cu (II) by coir pith carbon. *J. Chemosphere* **34**, 377–399.

Odoemelam, S. A., Emeh, U. N. & Eddy, N. O. 2018 Experimental and computational chemistry studies on the removal of methylene blue and malachite green dyes from aqueous solution by neem (Azadirachta indica) leaves. *J. Taibah Univ. Sci.* **12**(3), 255–265.

Parthasarathy, S., Manju, N., Hema, M. & Arivoli, S. 2011 Removal of malachite green from industrial waste-water by activated carbon prepared from cashew nut bark Alfa Universal. *Int. J. Chem.* **2**(2), 41.

Romero-Gonzalez, J., Peralta-Videa, J. R., Rodriguez, E., Ramirez, S. L. & Gardea-orresdey, J. L. 2005 Determination of thermodynamic parameters of Cr(VI) adsorption from aqueous solution onto Agave lechuguilla biomass. *J. Chem. Thermodyn.* **37**, 343–347.

Saha, P., Chowdhury, S., Gupta, S. & Kumar, I. 2010a Insight into adsorption equilibrium, kinetics and thermodynamics of Malachite Green onto clayey soil of Indian origin. *Chem. Eng. J.* **165**, 874–882.

Saha, P., Chowdhury, S., Gupta, S., Kumar, I. & Kumar, R. 2010b Assessment on the removal of malachite green using tamarind fruit shell as biosorbent. *Clean Soil Air Water* **38**(5–6), 437.

Santhi, T., Manonmani, S. & Smitha, T. 2010 Removal of malachite green from aqueous solution by activated carbon prepared from the epicarp of Ricinus communis by adsorption. *J. Hazard. Later* **179**, 178.

Santhi, T., Manonmani, S., Vasatha, V. & Chang, Y. 2011 A new alternative adsorbent for the removal of cationic dues from aqueous solutions. *Arab. J. Chem.* **9**, 466–474.

Sekhar, C. P., Kalidhasan, S., Rajesh, V. & Rajesh, N. 2009 Biopolymer adsorbent for the removal of malachite green from aqueous solution. *Chemosphere* **77**, 842.

Sen, S. K., Raut, S., Dora, T. K. & Mohapatra, P. K. D. 2014 Contribution of hot spring bacterial consortium in cadmium and lead bioremediation through quadratic programming model. *J. Hazard. Mater.* **265**, 47–60.

Sharma, Y. C., Uma, A., Sinha, A. S. K. & Upadhyay, S. N. 2010 Characterization and adsorption studies of Cocos nucifera L. activated carbon for the removal of methylene blue from aqueous solutions. *J. Chem. Eng.* **55**, 2662–2667.

Srivastava, S., Sinha, R. & Roy, D. 2004 Toxicological effects of malachite green. *Aquat. Toxicol.* **66**, 319–329.

Sujitha, R. & Ravindhranath, K. 2017a Defluoridation studies using active carbon derived from the barks of Ficus racemosa plant. *J. Fluor. Chem.* **19**, 358–366.

Sujitha, R. & Ravindhranath, K. 2017b Extraction of phosphate from polluted waters using calcium alginate beads doped with active carbon derived from Achyranthes aspera plant as adsorbent. *J. Anal. Methods Chem.* **2017**, 13. Article ID: 3610878.

Sujitha, R. & Ravindhranath, K. 2018a Removal of lead (II) from wastewater using active carbon of caryota urens seeds and its embedded calcium alginate beads as adsorbents. *J. Environ. Chem. Eng.* **6**, 4298–4309.

Sujitha, R. & Ravindhranath, K. 2018b Effective removal of Methylene blue, a hazardous dye from industrial effluents using active carbon of barks of F. infectoria plant. *Int. J. Environ. Sci. Technol.* https://doi.org/10.1007/s13762-018-2147-3.

Sujitha, R. & Ravindhranath, K. 2018c Enhanced removal of chromium (VI) from waste water using active carbon derived from Lantana camara plant as adsorbent. *Water Sci. Technol.* **78**(6), 1377–1389.

Temkin, M. J. & Pyzhev, V. 1940 Recent modifications to Langmuir isotherms. *Acta Physiochim* **12**, 217–222.

Tsai, W. T. & Chen, H. R. 2010 Removal of malachite green from aqueous solution using low-cost chlorella-based biomass. *J. Hazard. Mater.* **175**, 844.

Uma, Banerjee, S. & Sharma, Y. C. 2013 Equilibrium and kinetic studies for removal of malachite green from aqueous solution by a low cost activated carbon. *J. Ind. Eng. Chem.* **19**, 1099–1105.

Yadav, S., Srivastava, V., Banerjee, S., Weng, C. H. & Sharma, Y. S. 2013 Adsorption characteristics of modified sand for the removal of hexavalent chromium ions from aqueous solutions: kinetics, thermodynamic and equilibrium studies. *Catena* **100**, 120–127.

Yonar, M. E. & Yonar, S. M. 2010 Changes in selected immunological parameters and antioxidant status of rainbow trout exposed to malachite green. *Pestic. Biochem. Physiol.* **97**(1), 19.

Yu, M., Han, Y., Li, J. & Wang, L. 2017 CO_2-activated porous carbon derived from cattail biomass for removal of malachite green dye and application as super capacitors. *Chem. Eng. J.* **317**, 493–502.

Zhang, J., Li, Y., Zhang, C. & Jing, Y. 2008 Adsorption of malachite green from aqueous solution onto carbon prepared from Arundo donax root. *J. Hazard. Mater.* **50**, 774.